

Electro, Physical & Theoretical Chemistry

Theoretical Studies on Reactions of OH with $\text{H}_2\text{SO}_4 \cdots \text{NH}_3$ Complex and NH_2 with H_2SO_4 in the Presence of WaterBo Long,^{*[a]} Xing-Feng Tan,^[a] Yi-Bo Wang,^[c] Jun Li,^[b] Da-Sen Ren,^[a] and Wei-Jun Zhang^[d, e]

The OH + $\text{H}_2\text{SO}_4 \cdots \text{NH}_3$, $\text{NH}_2 + \text{H}_2\text{SO}_4$, and $\text{NH}_2 + \text{H}_2\text{SO}_4 \cdots \text{H}_2\text{O}$ reactions have been theoretically investigated using high-accuracy quantum chemical methods and conventional transition state theory. The calculation results reveal that remarkable tunneling effects appear at 200 K in the OH + $\text{H}_2\text{SO}_4 \cdots \text{NH}_3$ reaction, compared with obvious tunneling effects below 100 K in the OH + NH_3 reaction. The calculated rate constants predict that the hydrogen atom of the free OH group in M1 ($\text{H}_2\text{SO}_4 \cdots \text{NH}_3$) abstracted via OH can compete well with the H atom in H_2SO_4

abstracted by OH at 200–240 K. The reaction kinetic results also show that a single water molecule could play an important role in the $\text{NH}_2 + \text{H}_2\text{SO}_4 \cdots \text{H}_2\text{O}$ reaction below 240 K. The present results provide new insights into the atmospheric oxidation of sulfuric acid, which could be of great use in understanding atmospheric nucleation processes. Additionally, the findings are tunneling effects enhanced by sulfuric acid, which may be wide applications in reaction kinetics of gas-phase reactions.

1. Introduction

The vital significance of sulfuric acid in the atmosphere is due to the main contributor to acid rain^[1] and the most important nucleation precursor of atmospheric aerosols.^[2–11] Atmospheric aerosols play critical roles in climate change.^{[12–14][15]} In addition, they have adverse influences on human health.^[16–18] At the beginning of the formation for atmospheric sulfate aerosols at a molecular level, sulfuric acid interacts with atmospheric molecules such as water, ammonia, and amines responsible for the formation of sulfuric acid-containing clusters.^[2,5,6,9–11,19–21] Exploring reactivities of sulfuric acid-containing clusters is of key necessity for fully elucidating the fates of atmospheric molecules and understanding the nucleation processes of sulfate aerosols from the molecular level of view.

Sulfuric acid and NH_3 can form a hydrogen-bonded $\text{H}_2\text{SO}_4 \cdots \text{NH}_3$ complex, which has been widely studied by both experimental and theoretical methods^[22–25] because of the im-

portant roles of H_2SO_4 or $\text{H}_2\text{SO}_4 \cdots \text{NH}_3$ in nucleation processes of atmospheric aerosols.^[5,21,26–28] It is noted that the interaction between sulfuric acid and ammonia is much stronger than that of the corresponding sulfuric acid and H_2O by 4–5 kcal/mol.^[29,30] The stronger interaction between H_2SO_4 and NH_3 could lead to the possible existence of the $\text{H}_2\text{SO}_4 \cdots \text{NH}_3$ complex under atmospheric conditions. Additionally, the atmospheric nucleation precursor such as sulfuric acid also affects radical-molecule reactions such as OH + HCHO^[31] and OH + CH_3OH .^[32] On the other hand, it is worth mentioning that the rate constant (between 1.47×10^{-13} and 1.60×10^{-13} $\text{cm}^3 \text{ molecule}^{-1} \text{ s}^{-1}$) of OH + NH_3 ^[33–36] is 10 times faster than that of OH + H_2SO_4 .^[37] When there are OH, NH_3 , and H_2SO_4 coexistent in the atmosphere, the reaction of OH with NH_3 is preferred over the OH + H_2SO_4 reaction, resulting in the formation of NH_2 . Such processes are similar to the atmospheric oxidation of HNO_3 ^[38,39] when OH, NH_3 , and HNO_3 exist simultaneously in the atmosphere. Thus, studying the title reactions is of great interest for clarifying the atmospheric oxidation of sulfuric acid in Earth's chemistry.

Herein, this is the first investigation on the reaction of OH with $\text{H}_2\text{SO}_4 \cdots \text{NH}_3$ complex and the reaction of sulfuric acid with NH_2 in the presence of water using high-accuracy quantum chemical methods and transition state theory. These investigations are crucial because the ammonia is the prototype of amines as nucleation precursors which make important contributions to the formation of atmospheric aerosols.^[9] We explore whether ammonia can accelerate the OH + H_2SO_4 reaction and a single water molecule can promote the $\text{NH}_2 + \text{H}_2\text{SO}_4$ reaction. Some theoretical and experimental investigations have demonstrated that a single water molecule can affect the rate constants of gas-phase reactions in the atmosphere.^[40–58] In addition, the competition mechanisms between OH + NH_3 and OH + H_2SO_4 are also considered, which may be of great interest because previous investigations have demonstrated that the similar reaction mechanisms play an important role in the

[a] Prof. B. Long, X.-F. Tan, Prof. Dr. D.-S. Ren
College of Information Engineering, Guizhou Minzu University, Guiyang, 550025, China
E-mail: longbo@gzmu.edu.cn

[b] Prof. Dr. J. Li
Department of Chemistry & Laboratory of Organic Optoelectronics and Molecular Engineering of the Ministry of Education, Tsinghua University, Beijing 100084, China

[c] Prof. Y.-B. Wang
Key Laboratory of Guizhou High Performance Computational Chemistry, Department of Chemistry, Guizhou University, Guiyang, 550025, China

[d] Prof. Dr. W.-J. Zhang
Laboratory of Atmospheric Physico-Chemistry, Anhui Institute of Optics and Fine Mechanics, Chinese Academy of Sciences, Hefei, 230031, China

[e] Prof. Dr. W.-J. Zhang
Key Laboratory of Atmospheric Composition and Optical Radiation, Anhui Institute of Optics and Fine Mechanics, Chinese Academy of Sciences, Hefei, 230031, China

Supporting information for this article is available on the WWW under <http://dx.doi.org/10.1002/slct.201600194>

Table 1. The Binding, Activated, and Reaction enthalpies (ΔH), free energies (ΔG), and energies (ΔE) for the reactions of OH with $H_2SO_4 \cdots NH_3$ and NH_2 with H_2SO_4 with zero-point correction (ZPE) included at 298 K. (in kcal/mol).

	M06-2X			CCSD(T) // M06-2X		
	ΔH	ΔG	ΔE	ΔH	ΔG	ΔE
$H_2SO_4 + NH_3 + OH \longrightarrow H_2SO_4 \cdots NH_2 \cdots H_2O$						
$H_2SO_4 + NH_3 + OH$	0.00	0.00	0.00	0.00	0.00	0.00
M1 ($H_2SO_4 \cdots NH_3$) + OH	-16.35	-8.00	-15.84	-15.42	-7.07	-14.91
C1	-25.62	-8.69	-24.48	-23.65	-6.71	-22.50
TS1 A	-13.98	4.43	-12.29	-11.33	7.08	-9.64
TS1B	-17.84	0.14	-16.61	-14.65	3.33	-13.41
M1 A	-31.99	-16.31	-31.26	-31.31	-15.63	-30.58
$H_2SO_4 + NH_3 + OH \longrightarrow HSO_4 \cdots NH_3 \cdots H_2O$						
CN1 ($NH_3 \cdots H_2SO_4 \cdots OH$)	-26.29	-9.16	-25.03	-24.51	-7.38	-23.25
TSN1	-16.21	2.32	-14.33	-13.22	5.31	-11.35
TSN2	-16.56	1.97	-14.68	-13.52	5.00	-11.64
TSN3	-14.95	2.81	-13.93	-12.03	5.73	-10.47
TSN4	-18.71	0.25	-16.57	-15.05	3.92	-12.90
CN1P	-25.79	-11.23	-25.48	-25.97	-11.41	-25.66
FN1P ($NH_3 \cdots HSO_4$) + H_2O	-23.36	-23.07	-22.64	-23.53	-15.82	-23.10
$HSO_4 + NH_2 \longrightarrow HSO_4 + NH_3$						
$H_2SO_4 + NH_2$	0.00	0.00	0.00	0.00	0.00	0.00
C2 A	-11.97	-3.73	-11.50	-11.35	-3.12	-10.88
TS2 A1	-5.73	4.08	-5.58	-4.99	4.83	-3.83
TS2 A2	-0.60	8.77	0.36	0.06	9.53	1.01
C2B	-6.35	2.74	-5.64	-4.02	5.07	-3.31
TS2B	-0.66	8.62	0.12	0.68	9.96	1.46
C2P	-12.23	-3.62	-11.52	-12.34	-3.74	-11.63
$HSO_4 + NH_3$	5.85	5.37	5.92	4.40	3.92	4.47
$H_2SO_4 + H_2O + NH_2 \longrightarrow HSO_4 \cdots NH_3 \cdots H_2O$						
$H_2SO_4 + H_2O + NH_2$	0.00	0.00	0.00	0.00	0.00	0.00
M2 ($H_2SO_4 \cdots H_2O$) + NH_2	-12.31	-3.44	-11.58	-11.43	-2.56	-10.70
M3 ($H_2O \cdots NH_2$) + H_2SO_4	-3.46	2.33	-3.05	-3.52	2.26	-3.11
CW1 A	-21.36	-4.52	-20.19	-19.38	-2.53	-18.20
TSW1 A	-17.44	2.92	-15.16	-13.82	6.55	-11.54
TSWR	-14.81	1.79	-14.18	-12.39	4.20	-11.76
CW1B	-16.73	1.51	-15.39	-14.70	3.53	-13.36
TSW1B	-8.24	10.14	-6.81	-6.78	11.60	-5.36
CW1P	-22.81	-4.75	-21.27	-23.86	-5.79	-22.31
M1 A	-21.15	-4.57	-20.14	-20.13	-3.55	-19.12
TSW2 A	-17.66	1.78	-15.77	-16.29	3.15	-14.40
CW2B	-17.06	1.57	-15.64	-14.17	4.46	-12.74
TSW2B	-14.45	4.80	-12.78	-11.54	7.71	-9.87
CW2C	-16.73	2.52	-15.08	-13.40	5.84	-11.76
TSW2C	-11.26	6.41	-10.26	-10.13	7.54	-9.13
CW2P	-23.01	-4.79	-21.43	-23.91	-5.68	-22.33

which agrees well with the value of 1.603 Å at the CCSD(T)-F12 A/VDZ-F12 level as shown in Figure S1 (Supporting Information). In Table 1, it is noted that the binding energy of the M1 complex is evaluated to be -14.91 kcal/mol at the CCSD(T)/aug-cc-pv(T+d)z//M06-2X/6-311++G(3df,3pd) level, which is in reasonable agreement with the data of -14.49 kcal/mol at the CCSD(T)-F12B/VQZ-F12//CCSD(T)-F12 A/VDZ-F12 level as listed in Table S1 (Supporting Information). Although the binding Gibbs free energy (ΔG (298 K)) of the M1 ($H_2SO_4 \cdots NH_3$) complex is computed to be -7.07 kcal/mol at the CCSD(T)/aug-cc-pv(T+d)z//M06-2X/6-311++G(3df,3pd) level, which is 1.37 kcal/mol lower than that computed by the CCSD(T)-F12B/VQZ-F12//CCSD(T)-F12 A/VDZ-F12 method, the value is not outside of the range from -4.5 to -9.2 kcal/mol in the literature.^[21,22,2930] Additionally, the enthalpy change (-15.42 kcal/mol) at 298 K at the CCSD(T)/aug-cc-pv(T+d)z//M06-2X/6-311++G(3df,3pd) level agrees reasonably with the experimental value of -16.1 ± 0.6 kcal/mol.^[59] Regarding the M2 ($H_2SO_4 \cdots H_2O$) complex, the benchmark calculations show that the binding energy and binding free energy of

atmospheric oxidation of HNO_3 .^[38,39] Therefore, our investigation should provide new insights into the atmospheric evolution of sulfuric acid relative to nucleation processes of atmospheric aerosols.

2. Results and Discussion

2.1. The $H_2SO_4 \cdots NH_3$ and $H_2SO_4 \cdots H_2O$ complexes

The M1 ($H_2SO_4 \cdots NH_3$) and M2 ($H_2SO_4 \cdots H_2O$) complexes are re-investigated to estimate the error bar of theoretical methods used herein and the importance of the two complexes in the atmosphere. The M1 ($H_2SO_4 \cdots NH_3$) binary complex is stabilized by the hydrogen-bonded interaction between the hydrogen atom in H_2SO_4 and the nitrogen atom in NH_3 with the N...H distance of 1.548 Å at the M06-2X/6-311++G(3df,3pd) level,

-10.70 kcal/mol and -2.56 kcal/mol calculated by CCSD(T)/aug-cc-pv(T+d)z//M06-2X/6-311++G(3df,3pd) are consistent with those of -10.27 kcal/mol and -2.13 kcal/mol computed by CCSD(T)-F12B/VQZ-F12//CCSD(T)-F12 A/VDZ-F12, respectively. Moreover, the binding free energy of M2 ($H_2SO_4 \cdots H_2O$) is computed to be -2.56 kcal/mol at the CCSD(T)/aug-cc-pv(T+d)z//M06-2X/6-311++G(3df,3pd) level, which agrees well with the experimental value of -3.6 ± 1 kcal/mol.^[60] The results indicate that the CCSD(T)/aug-cc-pv(T+d)z//M06-2X/6-311++G(3df,3pd) method has an error bar of about 1–2 kcal/mol.

To estimate the importance of the $H_2SO_4 \cdots NH_3$ and $H_2SO_4 \cdots H_2O$ complexes in the atmosphere, the corresponding equilibrium constants are calculated as shown in Table 2. The concentration ratio of $H_2SO_4 \cdots NH_3$ and $H_2SO_4 \cdots H_2O$ is written in eq (1).

Table 2. The equilibrium constant (K_{eq} , molecule cm^{-3}) and the unimolecular rate constant (k , s^{-1}) for the individual reaction pathway with the temperature range 200–298 K*.

Reaction	200 K	220 K	240 K	260 K	280 K	298 K
$K_{\text{eq}}(\text{H}_2\text{SO}_4 \cdots \text{NH}_3)$	1.51×10^{-9}	4.84×10^{-11}	2.77×10^{-12}	2.48×10^{-13}	3.16×10^{-14}	6.30×10^{-15}
$K_{\text{eq}}(\text{H}_2\text{SO}_4 \cdots \text{H}_2\text{O})$	2.71×10^{-14}	2.17×10^{-15}	2.67×10^{-16}	4.56×10^{-17}	1.01×10^{-17}	3.10×10^{-18}
$K_{\text{eq}3}$	1.36×10^{-17}	2.28×10^{-18}	5.16×10^{-19}	1.48×10^{-19}	5.11×10^{-20}	2.22×10^{-20}
k_4	1.06×10^3	2.05×10^3	4.08×10^3	8.25×10^3	1.69×10^4	3.23×10^4
k_{1A}	1.32×10^2	1.10×10^3	6.54×10^3	2.97×10^4	1.09×10^5	3.06×10^5
k_{1B}	8.36×10^{-17}	1.16×10^{-17}	2.24×10^{-18}	5.61×10^{-19}	1.72×10^{-19}	6.82×10^{-20}
$K_{\text{eq}N3}$	2.71×10^2	7.84×10^2	2.26×10^3	6.40×10^3	1.73×10^4	4.06×10^4
k'_{N1}	6.11×10^2	1.67×10^3	4.57×10^3	1.23×10^4	3.18×10^4	7.17×10^4
k'_{N2}	3.24×10^4	5.73×10^4	1.03×10^5	1.86×10^5	3.43×10^5	6.01×10^5
k'_{N3}	2.40×10^3	7.14×10^3	2.02×10^4	5.39×10^4	1.34×10^5	2.86×10^5
k'_{N4}	93.1	88.9	83.5	77.5	71.9	67.8
Γ_1	93.1	88.9	83.5	77.5	71.9	67.8
$K_{\text{eq}}(\text{H}_2\text{SO}_4 \cdots \text{NH}_2)$	6.70×10^{-14}	5.38×10^{-15}	6.64×10^{-16}	1.14×10^{-16}	2.55×10^{-17}	7.89×10^{-18}
k_7	5.82×10^{-2}	1.01×10^0	1.09×10^1	8.22×10^1	4.64×10^2	1.81×10^3
$k_{\text{NH}_2 + \text{H}_2\text{SO}_4}$	3.90×10^{-15}	5.43×10^{-15}	7.26×10^{-15}	9.39×10^{-15}	1.18×10^{-14}	1.43×10^{-14}
$K_{\text{eq}10}$	1.94×10^{-17}	3.40×10^{-18}	8.05×10^{-19}	2.40×10^{-19}	8.57×10^{-20}	3.84×10^{-20}
k_{11}	1.03×10^1	1.08×10^2	6.69×10^2	4.10×10^3	1.73×10^4	5.38×10^4
$K_{\text{eq}}(\text{H}_2\text{SO}_4 \cdots \text{OH})$	3.83×10^{-16}	5.27×10^{-17}	1.02×10^{-17}	2.55×10^{-18}	7.82×10^{-19}	3.11×10^{-19}
$k_{2(\text{TSS}1)}$	1.88×10^2	6.61×10^2	2.16×10^3	6.59×10^3	1.86×10^4	4.44×10^4
$k_{2(\text{TSS}2)}$	6.13×10^2	1.93×10^3	5.70×10^3	1.58×10^4	4.09×10^4	9.08×10^4
$k_{2(\text{TSS}3)}$	1.02×10^3	2.50×10^3	5.77×10^3	1.28×10^4	2.73×10^4	5.26×10^4
$k_{2(\text{TSS}4)}$	1.18×10^2	5.62×10^2	2.32×10^3	8.31×10^3	2.60×10^4	6.55×10^4
Γ_2	93.9	90.0	85.5	80.9	76.9	74.2
$k_{\text{OH} + \text{H}_2\text{SO}_4}$	7.44×10^{-13}	2.98×10^{-13}	1.62×10^{-13}	1.11×10^{-13}	8.82×10^{-14}	7.89×10^{-14}
v_3/v_2	$1.38 \times 10^{-15}[\text{H}_2\text{O}]$	$1.46 \times 10^{-16}[\text{H}_2\text{O}]$	$2.28 \times 10^{-17}[\text{H}_2\text{O}]$	$4.78 \times 10^{-18}[\text{H}_2\text{O}]$	$1.27 \times 10^{-18}[\text{H}_2\text{O}]$	$4.49 \times 10^{-19}[\text{H}_2\text{O}]$
$v_1/v_{(\text{OH} + \text{H}_2\text{SO}_4)}$	$3.29 \times 10^{-11}[\text{NH}_3]$	$1.17 \times 10^{-11}[\text{NH}_3]$	$9.37 \times 10^{-12}[\text{NH}_3]$	$1.26 \times 10^{-12}[\text{NH}_3]$	$2.31 \times 10^{-15}[\text{NH}_3]$	$6.00 \times 10^{-16}[\text{NH}_3]$
$v_{N1}/v_{(\text{OH} + \text{H}_2\text{SO}_4)}$	$5.94 \times 10^{-9}[\text{NH}_3]$	$1.21 \times 10^{-10}[\text{NH}_3]$	$4.70 \times 10^{-12}[\text{NH}_3]$	$3.03 \times 10^{-13}[\text{NH}_3]$	$2.94 \times 10^{-14}[\text{NH}_3]$	$4.83 \times 10^{-15}[\text{NH}_3]$

* Branching Ratios ($\Gamma_1 = (k_{N1} + k_{N2} + k_{N3}) / (k_{N1} + k_{N2} + k_{N3} + k_{N4})$ and $\Gamma_2 = (k_{2(\text{TSS}1)} + k_{2(\text{TSS}2)} + k_{2(\text{TSS}3)}) / (k_{2(\text{TSS}1)} + k_{2(\text{TSS}2)} + k_{2(\text{TSS}3)} + k_{2(\text{TSS}4)})$). k_{N1} , k_{N2} , k_{N3} , and k_{N4} standing for the rate constants of unimolecular reactions via the transition state TSN1, TSN2, TSN3, and TSN4 in Figure 2, respectively.

$$\frac{[\text{H}_2\text{SO}_4 \cdots \text{NH}_3]}{[\text{H}_2\text{SO}_4 \cdots \text{H}_2\text{O}]} = \frac{K_{\text{eq}}(\text{H}_2\text{SO}_4 \cdots \text{NH}_3) [\text{H}_2\text{SO}_4] [\text{NH}_3]}{K_{\text{eq}}(\text{H}_2\text{SO}_4 \cdots \text{H}_2\text{O}) [\text{H}_2\text{SO}_4] [\text{H}_2\text{O}]} = \frac{K_{\text{eq}}(\text{H}_2\text{SO}_4 \cdots \text{NH}_3) [\text{NH}_3]}{K_{\text{eq}}(\text{H}_2\text{SO}_4 \cdots \text{H}_2\text{O}) [\text{H}_2\text{O}]} \quad (1)$$

The concentration of ammonia is reported in the range between 1.16×10^{10} and 1.32×10^{12} molecule cm^{-3} .^[61,62] The ratio of $K_{\text{eq}}(\text{H}_2\text{SO}_4 \cdots \text{NH}_3)$ and $K_{\text{eq}}(\text{H}_2\text{SO}_4 \cdots \text{H}_2\text{O})$ is about 1.04×10^4 at 240 K. When the upper limit concentration for ammonia is 1.32×10^{12} molecule cm^{-3} , the $\text{H}_2\text{SO}_4 \cdots \text{NH}_3$ complex could only compete well with the $\text{H}_2\text{SO}_4 \cdots \text{H}_2\text{O}$ complex at 240 K with the upper limit concentration of water about 1.37×10^{16} molecule cm^{-3} .

2.2. Reaction between OH and $\text{H}_2\text{SO}_4 \cdots \text{NH}_3$

OH radical reacts with the M1 ($\text{H}_2\text{SO}_4 \cdots \text{NH}_3$) complex as depicted in Figure 1. The optimized geometries are presented in Figure S1 (Supporting Information). There are two main reaction processes, depending on that OH approaches the hydrogen atom of NH_3 or the hydrogen atom of the free OH group of sulfuric acid in the M1 ($\text{H}_2\text{SO}_4 \cdots \text{NH}_3$) complex. OH attacks NH_3 in the M1 ($\text{H}_2\text{SO}_4 \cdots \text{NH}_3$) complex via the two reaction channels TS1 A and TS1B. OH begins with the formation of pre-reactive ternary complex C1 and undergoes two different transition states TS1 A and TS1B responsible for the formation of the complex M1 A. The C1 complex is formed via strong hydrogen-bonded interactions with the binding energy of -22.50 kcal/mol relative to the separate reactants OH, NH_3 , and H_2SO_4 . C1 is transformed into M1 A by the transition state TS1 A, where OH

abstracts the hydrogen atom of NH_3 in M1 ($\text{H}_2\text{SO}_4 \cdots \text{NH}_3$) and sulfuric acid is a spectator as shown in Figure 1. It is worth mentioning that TS1 A has an energy barrier of 5.27 kcal/mol relative to OH and M1 ($\text{H}_2\text{SO}_4 \cdots \text{NH}_3$), which is about 2 kcal/mol higher than that (3.20 kcal/mol) of the naked OH + NH_3 reaction at the CCSD(T)/aug-cc-pv(T+d)z//M06-2X/6-311 + + G (3df,3pd) level. The energy barrier of the OH + NH_3 reaction is estimated to be 3.20 kcal/mol herein, which is consistent with the value of about 3.3 kcal/mol at the CCSD(T)(FULL)/aug-cc-pVTZ//CCSD(T)(FC)/cc-pVTZ level.^[34,63] Of great interest is C1 transformed into M1 A via the rearrangement reaction, which occurs via TS1B. The detailed illustration of TS1B is provided in Figure S2 (Supporting Information), where intrinsic reaction coordinate calculation is presented to show the C1 conversion into M1 A. The transition state TS1B is formed due to the rotation of the N–H bond along the N···H bond axis. It is noted that the energy barrier via TS1B is computed to be about 1.5 kcal/mol with respect to OH and M1, which is about 3.8 kcal/mol lower than that of TS1 A. Moreover, the energy barrier of TS1 A (1.5 kcal/mol) is also lower than that of the naked OH + NH_3 reaction by about 1.7 kcal/mol. Therefore, the OH + M1 ($\text{H}_2\text{SO}_4 \cdots \text{NH}_3$) reaction could compete well with the OH + NH_3 reaction from an energetic point of view.

When OH attacks the free OH group in M1 ($\text{H}_2\text{SO}_4 \cdots \text{NH}_3$), the ternary CN1 complex is firstly formed via the hydrogen-bonded interactions with a binding energy of -23.50 kcal/mol relative to the separate reactants, which is about 0.75 kcal/mol lower

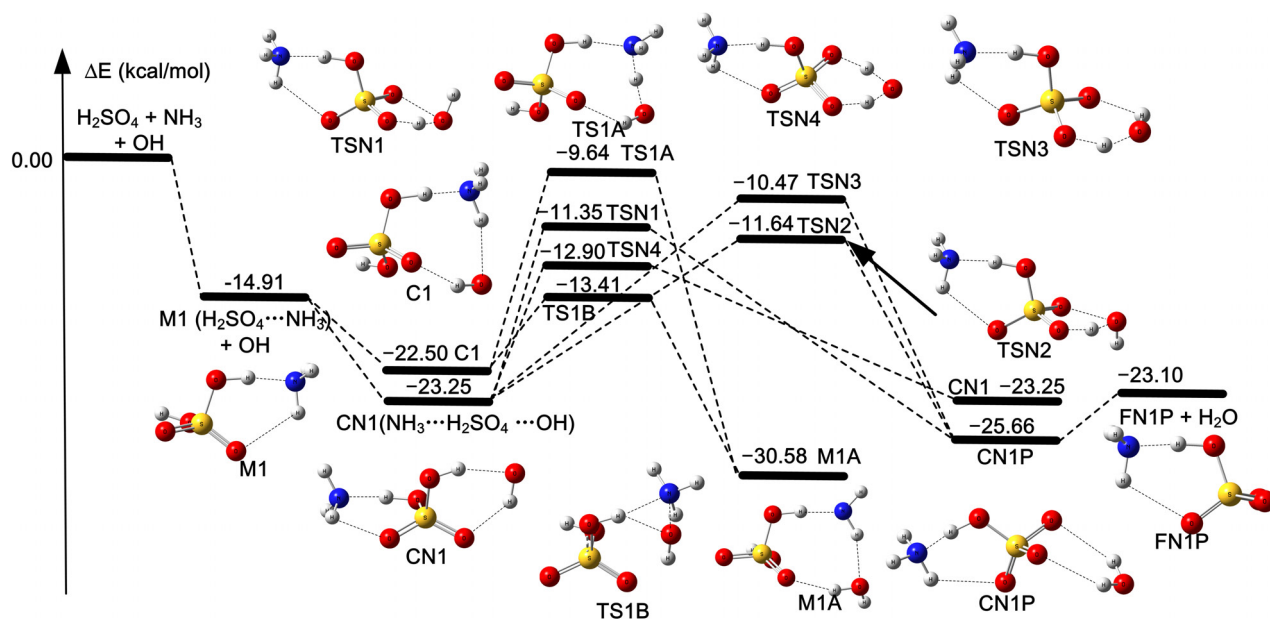


Figure 1. The calculated potential energy profile for the $\text{OH} + \text{H}_2\text{SO}_4 \cdots \text{NH}_3$ at the CCSD(T)/aug-cc-pv(T+d)z//M06-2X/6-311++G(3df,3pd) level of theory (in kcal/mol).

than that of C1. OH mainly abstracts the hydrogen atom of the free OH group of sulfuric acid in M1 ($\text{H}_2\text{SO}_4 \cdots \text{NH}_3$) via four different reaction channels (TSN1, TSN2, TSN3, and TSN4), which are similar to the processes in the reaction of OH with H_2SO_4 in the absence and presence of water.^[37,64] The analysis of natural orbital of TSN1 and TSN2 in Figure S3 (Supporting information) reveals that TSN1 and TSN2 are the proton-coupled electron transfer mechanisms, which are in accordance with the naked $\text{OH} + \text{H}_2\text{SO}_4$ reaction.^[37] From an energetic point of view, the dominant channel via TSN4 in the $\text{OH} + \text{M1}$ ($\text{H}_2\text{SO}_4 \cdots \text{NH}_3$) reaction is a double hydrogen transfer process with the lowest energy barrier of about 2 kcal/mol with respect to $\text{OH} + \text{M1}$ ($\text{H}_2\text{SO}_4 \cdots \text{NH}_3$), which is 0.3 kcal/mol lower than that of the corresponding $\text{OH} + \text{H}_2\text{SO}_4$ reaction (TSS4 in Table S2 of Supporting information) at the CCSD(T)/aug-cc-pv(T+d)z//M06-2X/6-311++G(3df,3pd) level. Additionally, the lowest energy barrier of the hydrogen abstraction via TSN2 in the $\text{OH} + \text{M1}$ ($\text{H}_2\text{SO}_4 \cdots \text{NH}_3$) reaction is estimated to be 3.27 kcal/mol with respect to OH and M1 ($\text{H}_2\text{SO}_4 \cdots \text{NH}_3$), which is slightly higher than that of the corresponding $\text{OH} + \text{H}_2\text{SO}_4$ reaction (TSS2 in Table S2 of Supporting Information) by about 0.5 kcal/mol. It is particularly noted that the reaction is exothermic due to the estimated reaction enthalpy of $\Delta H(298\text{ K}) = -8.11$ kcal/mol with respect to OH and M1 ($\text{H}_2\text{SO}_4 \cdots \text{NH}_3$) as listed in Table 1. This is similar to the $\text{OH} + \text{H}_2\text{SO}_4 \cdots \text{H}_2\text{O}$ reaction in our previous investigation.^[64] Furthermore, the Gibbs free reaction energy is computed to be -15.82 kcal/mol at 298 K relative to free reactants OH, NH_3 , and H_2SO_4 , uncovering that the reaction is thermodynamically feasible.

2.3. Reactions of NH_2 with H_2SO_4 and $\text{H}_2\text{SO}_4 \cdots \text{H}_2\text{O}$

The Reaction of H_2SO_4 with NH_2 occurs via the two different transition states TS2 A1 and TS2 A2 responsible for the formation of C2B. Both transition states correspond to the common the pre-reactive complex C2 A as shown in Figure 2. The similar mechanism in the initial step of the $\text{NH}_2 + \text{H}_2\text{SO}_4$ reaction has also been found in the $\text{NH}_2 + \text{HNO}_3$ reaction.^[38,39] The pre-reactive C2 A complex is formed via double hydrogen bondings, which is similar to sulfuric acid monohydrate complex.^[64–68] The $\text{O}-\text{H} \cdots \text{N}$ hydrogen-bonded distance in C2 A is calculated to be 1.675 Å, while the $\text{O} \cdots \text{H}-\text{N}$ is estimated to be 2.485 Å in Figure S4 (Supporting Information), which is in good agreement with the corresponding values reported in the literature.^[69] In Table 1, C2 A has a binding energy of -10.88 kcal/mol with respect to the separate reactants H_2SO_4 and NH_2 , which is close to the binding energy of -10.70 kcal/mol in the $\text{H}_2\text{SO}_4 \cdots \text{H}_2\text{O}$ complex at the CCSD(T)/aug-cc-pv(T+d)z//M06-2X/6-311++G(3df,3pd) level.^[67] It is worth noting that the binding energy between sulfuric acid and amidogen radical is stronger than that of the $\text{HNO}_3 \cdots \text{NH}_2$ complex by about 2.5 kcal/mol.^[38,39,69] The two transition states TS2 A1 and TS2 A2 are proton-coupled electron transfer and hydrogen atom transfer, respectively, which are revealed via the natural orbital analysis in Figure S3 (Supporting Information). These reaction processes are also similar to the reaction of nitric acid with amidogen radical.^[38,39] The proton-coupled electron transfer mechanisms have been found in the reactions such as $\text{OH} + \text{H}_2\text{SO}_4$,^[37] $\text{OH} + \text{HCOOH}$,^[70–72] and $\text{OH} + \text{HNO}_3$.^[73] Of great interest is that TS2 A1 lies 3.83 kcal/mol below the reactants, which is about 4 kcal/mol lower than that of the $\text{HNO}_3 + \text{NH}_2$ reaction,^[38,39] whereas TS2 A2 lies 1.01 kcal/mol above the reactants. The energy dif-

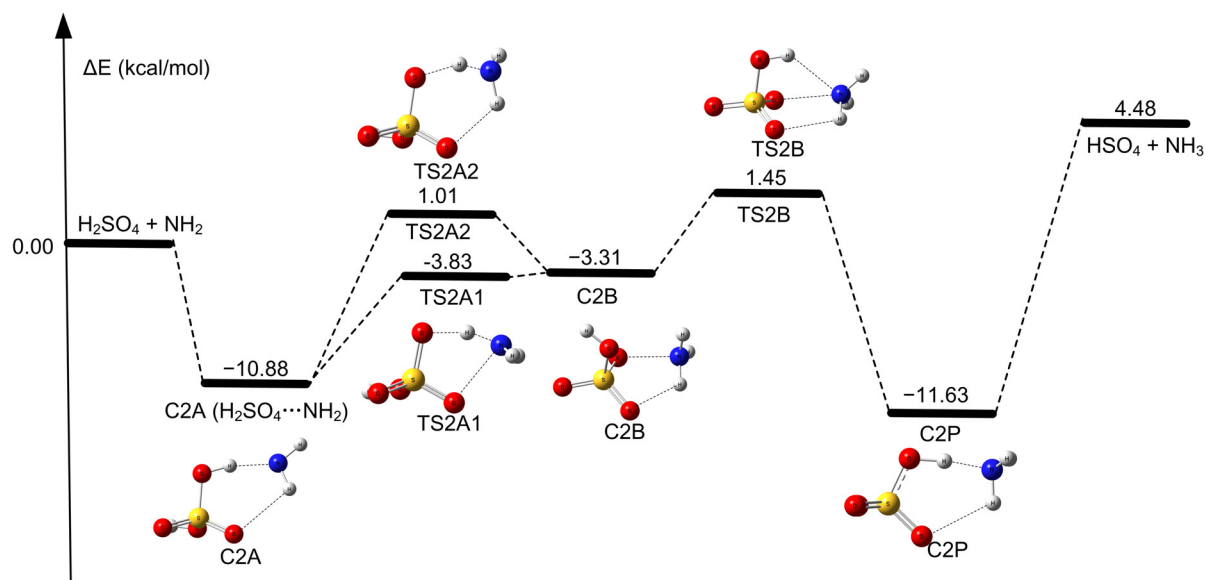


Figure 2. The calculated potential energy profile for the $\text{NH}_2 + \text{H}_2\text{SO}_4$ at the CCSD(T)/aug-cc-pv(T+d)z//M06-2X/6-311++G(3df,3pd) level of theory (in kcal/mol).

ference between TS2 A2 and TS2 A1 is 4.84 kcal/mol, which is similar to the value between nitric acid and amidogen radical.^[38,39] C2B proceeds through a rearrangement reaction via TS2B, leading to the formation of C2P as described in Figure 2. Note that the rate-determining step in the $\text{NH}_2 + \text{H}_2\text{SO}_4$ reaction is the rearrangement process via TS2B, whereas the rate-limiting step in the reaction of NH_2 with HNO_3 is the hydrogen atom abstraction of HNO_3 by NH_2 .^[38,39] In TS2B, the barrier height is computed to be 1.45 kcal/mol relative to the isolated reactants NH_2 and H_2SO_4 . The post-reactive complex C2P has a binding energy of -11.63 kcal/mol, which is about 1 kcal/mol lower than that of complex C2 A. It is noted that the products HSO_4 and NH_3 lie 4.47 kcal/mol above the reactants sulfuric acid and amidogen radical, which reflects the reaction is endothermic.

When the single water molecule is introduced into the $\text{H}_2\text{SO}_4 + \text{NH}_2$ reaction, the initial step is the formation of M2 ($\text{H}_2\text{SO}_4 \cdots \text{H}_2\text{O}$) or M3 ($\text{NH}_2 \cdots \text{H}_2\text{O}$). Since the binding energy of M2 ($\text{H}_2\text{SO}_4 \cdots \text{H}_2\text{O}$) is about 7.6 kcal/mol lower than that of M3 ($\text{NH}_2 \cdots \text{H}_2\text{O}$) in Table 1, the M3 ($\text{NH}_2 \cdots \text{H}_2\text{O}$) complex is negligible in the atmosphere. Therefore, we consider the $\text{NH}_2 + \text{M2}$ ($\text{H}_2\text{SO}_4 \cdots \text{H}_2\text{O}$) reaction as presented in Figure 3, Figure S4, Figure S5, and Figure S6 (Supporting Information), which is similar to the $\text{OH} + \text{HNO}_3$ and $\text{OH} + \text{HCOOH}$ reactions in the presence of water.^[71,73]

As for the $\text{NH}_2 + \text{M2}$ ($\text{H}_2\text{SO}_4 \cdots \text{H}_2\text{O}$) reaction, the first step is the interaction between the nitrogen atom in NH_2 and the hydrogen atom of H_2O or the OH group in M2 ($\text{H}_2\text{SO}_4 \cdots \text{H}_2\text{O}$). The corresponding reaction mechanisms are presented in Figure 3 and Figure S6. When NH_2 approaches near H_2O in M2 ($\text{H}_2\text{SO}_4 \cdots \text{H}_2\text{O}$), the pre-reactive CW1 A complex is formed via the interaction of the nitrogen atom in NH_2 with the hydrogen atom of H_2O in M2 ($\text{H}_2\text{SO}_4 \cdots \text{H}_2\text{O}$) as displayed in Figure 3. In Figure 3,

NH_2 can further abstract the hydrogen atom of water via the transition state TSW1 A responsible for the formation of CW1B. CW1B is transformed into CW1P via the transition state TSW1B. It is noted that the rate-determining step occurs in TSW1B, which is similar to the reaction of NH_2 with H_2SO_4 in Figure 2. Furthermore, the energy barrier is evaluated to be about 5.34 kcal/mol relative to $\text{OH} + \text{M2}$, which is about 4 kcal/mol higher than that of the $\text{NH}_2 + \text{H}_2\text{SO}_4$ reaction. The results show that a single water molecule does not accelerate the occurrence of interconversion between CW1B and CW1P. In addition, the CW1 A complex undergoes an unimolecular isomerization reaction (TSR), leading to the formation of M1 A, which is transformed into CW2P undergoes the transition states (TSW2 A, TSW2B, and TSW2C), wherein TSW2C is a rate-determining step with a barrier height of about 1.57 kcal/mol relative to $\text{OH} + \text{M2}$, which is about 3.8 kcal/mol lower than that of TSW1B. In TSW2 A, the H-atom of OH group in H_2SO_4 is extracted by NH_2 , where H_2O is acted as a catalyst. In TSW2B, the OH group rotates along the S–O single bond in sulfuric acid, leading to the formation of CW2C. In TSW2C, the rearrangement process occurs from the hydrogen bonding interaction between the hydrogen atom of OH group in HSO_4 and the oxygen atom of H_2O in CW2C to the stronger hydrogen-bonded complex formation between the hydrogen atom in HSO_4 and the nitrogen atom in NH_3 responsible for the formation of CW2P. The overall reaction process is thermodynamically favorable because the Gibbs free energy ΔG (298 K) is estimated to be -5.68 kcal/mol with respect to NH_2 , H_2SO_4 , and H_2O , where H_2SO_4 is converted into SO_4^- in the CW2P complex. The stepwise mechanism in hydrogen transfer processes has been observed in gas-phase reactions containing water clusters.^[74,75] In addition, when NH_2 extracts the hydrogen atom of OH group in M2, the reaction mechanisms are represented in Figure S6 (Supporting In-

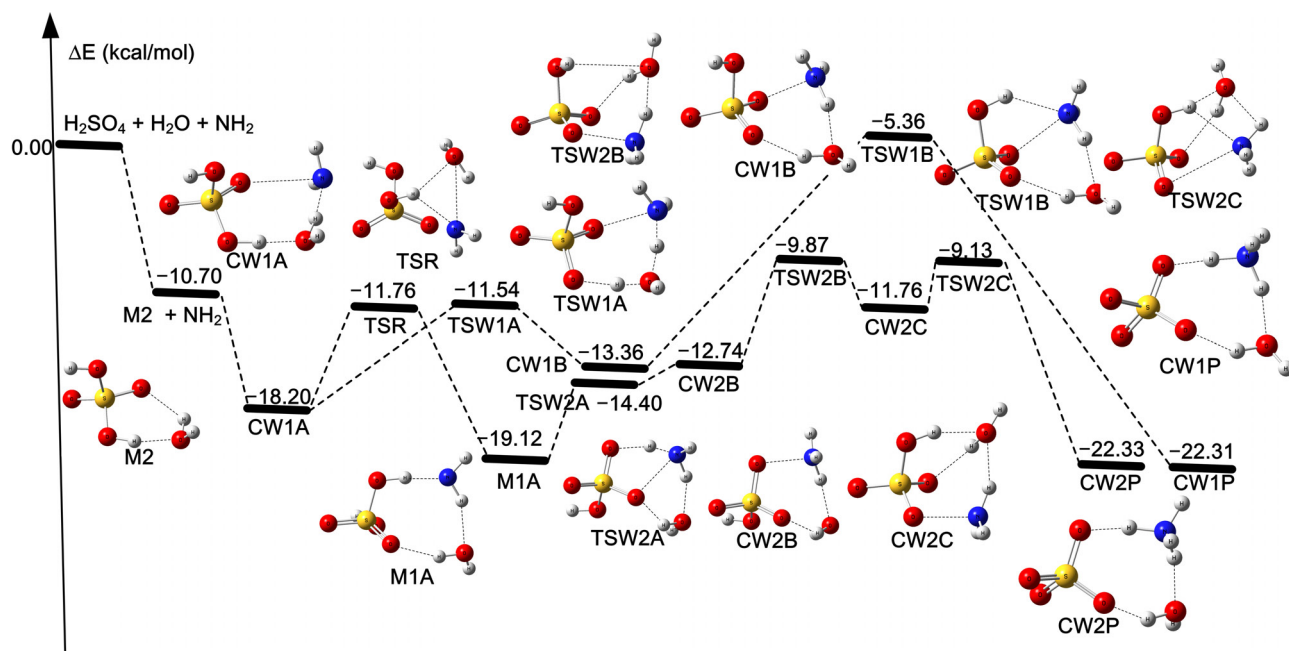


Figure 3. The calculated potential energy profile for the $\text{NH}_2 + \text{H}_2\text{SO}_4$ in the presence of water at the CCSD(T)/aug-cc-pv(T+d)z//M06-2X/6-311++G(3df,3pd) level of theory (in kcal/mol).

formation). The energy barrier of the rate-limiting step in Figure S6 is computed to be 3.79 kcal/mol with respect to $\text{OH} + \text{M}_2$, which is 2.22 kcal/mol higher than that of TSW2C in Figure 3. Thus, the process is of minor importance in the atmosphere.

2.4. Kinetics and Potential Applications in Atmospheric Chemistry

To determine the importance of these reactions investigated herein, the rate constants have been evaluated using conventional transition state theory. OH radical attacks the hydrogen atom of NH_3 in the M_1 ($\text{H}_2\text{SO}_4 \cdots \text{NH}_3$) complex is characterized along the potential energy profile of Figure 1 by eq (2)-(4).



The rate expression for the M_1A formation is obtained in eq (5a),

$$v_1 = \frac{d[\text{M}_1\text{A}]}{dt} = K_{\text{eq}(\text{H}_2\text{SO}_4 \cdots \text{NH}_3)} K_{\text{eq}3} k_4 [\text{H}_2\text{SO}_4] [\text{NH}_3] [\text{OH}] \quad (5a)$$

where the $K_{\text{eq}(\text{H}_2\text{SO}_4 \cdots \text{NH}_3)}$, $K_{\text{eq}3}$ are the equilibrium constants of the complex M_1 ($\text{H}_2\text{SO}_4 \cdots \text{NH}_3$) relative to $\text{H}_2\text{SO}_4 + \text{NH}_3$ in eq (2), and C_1 ($\text{H}_2\text{SO}_4 \cdots \text{NH}_3 \cdots \text{OH}$) with respect to $\text{H}_2\text{SO}_4 \cdots \text{NH}_3 + \text{OH}$ in

eq (3), respectively. k_4 is the unimolecular rate constant for C_1 transformation into M_1A via the transition states TS_1A and TS_1B in eq (4). The $[\text{H}_2\text{SO}_4]$, $[\text{NH}_3]$, and $[\text{OH}]$ are the concentrations of sulfuric acid, ammonia, and hydroxyl radical in the atmosphere, respectively. Similarly, we express the rate for the reaction route in Figure 1 responsible for the CN_1P and CN_1 formation in eq (5b),

$$v_{\text{N}1} = \frac{d[\text{CN}_1\text{P} + \text{CN}_1]}{dt} = K_{\text{eq}(\text{H}_2\text{SO}_4 \cdots \text{NH}_3)} K_{\text{eqN}3} k'_4 [\text{H}_2\text{SO}_4] [\text{NH}_3] [\text{OH}] \quad (5b)$$

where $K_{\text{eqN}3}$ is the equilibrium constant between the complex CN_1 and $\text{OH} + \text{M}_1$ ($\text{H}_2\text{SO}_4 \cdots \text{NH}_3$), and k'_4 is the unimolecular rate constant for CN_1 conversion into CN_1P and CN_1 in Figure 1.

As for the $\text{H}_2\text{SO}_4 + \text{NH}_2$ reaction, the main reaction steps can be expressed as in eq (6)-(7).



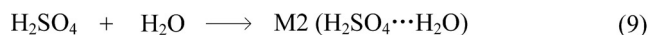
The rate can be obtained in terms of quasi-equilibrium approximations in eq (8).

$$v_2 = \frac{d[\text{C}_2\text{P}]}{dt} = K_{\text{eq}(\text{H}_2\text{SO}_4 \cdots \text{NH}_2)} k_7 [\text{H}_2\text{SO}_4] [\text{NH}_2] \quad (8)$$

Herein, we consider the C_2P intermediate as a possible re-

action end species because the reaction ($\text{H}_2\text{SO}_4 + \text{NH}_2 \longrightarrow \text{HSO}_4 + \text{NH}_3$) is endoergic, while the process ($\text{H}_2\text{SO}_4 + \text{NH}_2 \longrightarrow \text{C2P}$) is exoergic.

When the single water molecule is introduced into $\text{NH}_2 + \text{H}_2\text{SO}_4$, the dominant reaction pathway is that NH_2 approaches H_2O in the M2 ($\text{H}_2\text{SO}_4 \cdots \text{H}_2\text{O}$) complex in Figure 3 as characterized via eq (9)–(11).



The reaction steps lead to the rate expression as represented in eq (12),

$$v_3 = \frac{d[\text{CW2P}]}{dt} = K_{\text{eq}(\text{H}_2\text{SO}_4 \cdots \text{H}_2\text{O})} K_{\text{eq}10} k_{11} [\text{H}_2\text{SO}_4] [\text{NH}_2] [\text{H}_2\text{O}] \quad (12)$$

where $K_{\text{eq}10}$ is the ratio between the forward rate constant and reverse rate constant in eq (10) and k_{11} denotes the unimolecular rate constant of the CW1 A ($\text{H}_2\text{O} \cdots \text{H}_2\text{SO}_4 \cdots \text{NH}_2$) complex conversion to the CW2P.

The rate constants are provided in Table 2. The relative rate between $\text{OH} + \text{M1}$ ($\text{H}_2\text{SO}_4 \cdots \text{NH}_3$ and $\text{H}_2\text{SO}_4 + \text{OH}$) is rewritten in eq (13).

$$\frac{v_{\text{N1}} + v_1}{v_{\text{OH} + \text{H}_2\text{SO}_4}} = \frac{K_{\text{eq}(\text{H}_2\text{SO}_4 \cdots \text{NH}_3)} (K_{\text{eq}2} k'_4 + K_{\text{eq}2} k_4) [\text{NH}_3]}{K_{\text{OH} + \text{H}_2\text{SO}_4}} \quad (13)$$

The overall rate constant of the $\text{OH} + \text{H}_2\text{SO}_4$ reaction is also estimated to be $7.89 \times 10^{-14} \text{ cm}^3 \text{ molecule}^{-1} \text{ s}^{-1}$ at 298 K in Table 2, which is consistent with the value of $1.50 \times 10^{-14} \text{ cm}^3 \text{ molecule}^{-1} \text{ s}^{-1}$ in the literature.^[37] The concentration of ammonia is reported in the range between 1.16×10^{10} and $1.32 \times 10^{12} \text{ molecule cm}^{-3}$.^[61,62] Table 2 tells us that the $\text{OH} + \text{H}_2\text{SO}_4 \cdots \text{NH}_3$ reaction via transition states TSN1, TSN2, TSN3, and TSN4 can compete well with the reaction $\text{OH} + \text{H}_2\text{SO}_4$ at 200–240 K, while the reaction of $\text{OH} + \text{H}_2\text{SO}_4 \cdots \text{NH}_3$ is of minor importance above 240 K. In addition, OH radical attacks the hydrogen atom of NH_3 in M1 ($\text{H}_2\text{SO}_4 \cdots \text{NH}_3$), which can not compete well the naked $\text{OH} + \text{H}_2\text{SO}_4$ reaction because the ratio $v_1/v_{(\text{OH} + \text{H}_2\text{SO}_4)}$ is less than 1. However, it is also noted that the tunneling effect is obvious about 200–240 K for the rate-determining step of C1 conversion to M1 A via TS1 A in Figure 1, whereas the remarkably tunneling effect in naked $\text{OH} + \text{NH}_3$ reaction does not appear above 200 K in Table 3, which is similar to the $\text{OH} + \text{CH}_3\text{OH}$ reaction in the literature.^[76] Therefore, the present results also predict that sulfuric acid strengthens the tunneling effect in the reaction of OH with ammonia, which may have wide applications in gas-phase reaction kinetics. As for the reaction of NH_2 with sulfuric acid, the rate constant is estimated to be $1.43 \times 10^{-14} \text{ cm}^3 \text{ molecule}^{-1} \text{ s}^{-1}$ at 298 K, which is about 10 times slower than that of $\text{NH}_2 + \text{HNO}_3$ reaction.^[38] Additionally, the rate constant of the $\text{NH}_2 + \text{H}_2\text{SO}_4$ reaction ($1.43 \times 10^{-14} \text{ cm}^3 \text{ molecule}^{-1} \text{ s}^{-1}$) at 298 K is not also faster than that ($7.89 \times 10^{-14} \text{ cm}^3 \text{ molecule}^{-1} \text{ s}^{-1}$) of $\text{OH} + \text{H}_2\text{SO}_4$.^[37]

Table 3. Tunneling correction factors for the prereactive complex ($\text{OH} \cdots \text{NH}_3$) conversion into postreactive complex ($\text{NH}_2 \cdots \text{H}_2\text{O}$) in the $\text{OH} + \text{NH}_3$ reaction and C1 conversion into M1 A via the transition state TS1 A in the $\text{OH} + \text{H}_2\text{SO}_4 \cdots \text{NH}_3$ reaction.*

Temperature (K)	$\text{OH} \cdots \text{NH}_3 \longrightarrow \text{NH}_2 \cdots \text{H}_2\text{O}^a$	$\text{C1} \longrightarrow \text{M1A}^a$	$\text{C1} \longrightarrow \text{M1A}^b$	$\text{C1} \longrightarrow \text{M1A}^c$
200	1.36×10^1	9.67×10^4	5.58×10^5	4.45×10^6
220	9.06×10^0	9.79×10^3	4.86×10^4	3.51×10^5
240	6.62×10^0	1.66×10^3	7.05×10^3	4.54×10^4
260	5.18×10^0	4.18×10^2	1.52×10^3	8.62×10^3
280	4.26×10^0	1.44×10^2	4.48×10^2	2.21×10^3
298	3.69×10^0	6.75×10^1	1.85×10^2	8.06×10^2

*a, b, and c represent that the electronic calculations were performed at the CCSD(T)/aug-cc-pv(T+d)z//M06-2X/6-311++G(3df,3pd), CCSD(T)/aug-cc-pv(T+d)z//CAM-B3LYP/6-311++G(3df,3pd) and CCSD(T)/aug-cc-pv(T+d)z//MPW1 K/6-311++G(3df,3pd) levels, respectively.

The results show that the sulfuric acid can not be partly transformed into the $\text{HSO}_4 \cdots \text{NH}_3$ complex in the presence of NH_2 via a similar catalytic cycle suggested by Anglada et al.^[38] However, as for the water molecule introduced into the reaction, when the typical concentration is about $5.18 \times 10^{17} \text{ molecule cm}^{-3}$,^[66] the corresponding rate ratio is about 11 at 240 K. Therefore, the $\text{NH}_2 + \text{H}_2\text{SO}_4 \cdots \text{H}_2\text{O}$ reaction can complete well with the naked $\text{NH}_2 + \text{H}_2\text{SO}_4$ reaction at temperatures below 240 K. The formed $\text{HSO}_4 \cdots \text{NH}_3$ complex furthermore interacts with atmospheric molecules, which are involved in ion-mediated nucleation.^[77,78]

To determine the reliability of the kinetic data, we analyzed the possible error bars in these calculations. There are three main factors that cause the error bars in the kinetic calculations: electronic structure methods, variational effects of transition states, and tunneling correction. The electronic structure methods used could yield the error bar of 1–2 kcal/mol, which can not lead to the mistaken conclusions because of the error cancellation. As for the variational effects of transition state, although the variational transition state theory can improve the reaction kinetics, the variational effects of transition states are not obvious in the similar reactions such as $\text{OH} + \text{HCOOH}$, and $\text{OH} + \text{HCHO}$. Therefore, the main error bar originates from tunneling correction. The tunneling correction factors are remarkable in the hydrogen atom abstraction of NH_3 and H_2SO_4 in the $\text{OH} + \text{H}_2\text{SO}_4 \cdots \text{NH}_3$ and $\text{OH} + \text{H}_2\text{SO}_4$ reaction as listed in Table 3 and S3 (Supporting Information). In Table S3, as for the relative rate $v_{\text{N1}}/v_{\text{OH} + \text{H}_2\text{SO}_4}$, the results should be reliable because the difference in the tunneling correction factors between $\text{OH} + \text{H}_2\text{SO}_4$ (TSS1, TSS2, TSS3, and TSS4) and $\text{OH} + \text{H}_2\text{SO}_4 \cdots \text{NH}_3$ (TSN1, TSN2, TSN3, TSN4, and TS1 A) is not remarkable. The tunneling correction factors depend on the imaginary frequencies of transition states due to the Eckart tunneling correction. The imaginary frequency of the transition state is provided in Table S4. In Table 3, the results show that the different theoretical methods provide remarkable tunneling correction factors for C1 conversion into M1 A via TS1 A. The results show that the tunneling correction factors are very sensitive to the imaginary frequency of the transition state. Thus, although the absolute

values of the tunneling correction factors may be not reliable for C1 conversion into M1 A via TS1 A, the qualitative conclusion that sulfuric acid enhances the tunneling correction factors should be reliable.

3. Conclusions

In this article, we theoretically investigate the reactions of $\text{OH} + \text{H}_2\text{SO}_4 \cdots \text{NH}_3$, $\text{NH}_2 + \text{H}_2\text{SO}_4$, and $\text{NH}_2 + \text{H}_2\text{SO}_4 \cdots \text{H}_2\text{O}$. In the $\text{OH} + \text{H}_2\text{SO}_4 \cdots \text{NH}_3$ reaction, when OH attacks the hydrogen atom of NH_3 in $\text{H}_2\text{SO}_4 \cdots \text{NH}_3$ complex, the reaction can not compete well with the naked $\text{OH} + \text{H}_2\text{SO}_4$ reaction, which is of minor importance in the atmosphere. Moreover, the remarkable tunneling effect occurs at 200 K in the OH abstraction of hydrogen atom of ammonia in $\text{OH} + \text{H}_2\text{SO}_4 \cdots \text{NH}_3$ complex when sulfuric acid is acted as an observer, whereas the obvious tunneling effect occurs at 100 K in the naked $\text{OH} + \text{NH}_3$ reaction. Therefore, the results predict that although sulfuric acid do not exert a catalytic role in $\text{OH} + \text{NH}_3$ reaction from the energetical point of view, it has strong effects on tunneling effects, which enhance the reaction rates. Therefore, the present results could stimulate one to consider that some molecules affect the reaction kinetics via the tunneling effects in the gas phase reactions such as $\text{OH} + \text{CH}_3\text{OH}$. In addition, OH abstracts the hydrogen atom of the free OH group in M1 ($\text{H}_2\text{SO}_4 \cdots \text{NH}_3$), when the ammonia is a spectator. The process is preferable to the naked $\text{OH} + \text{H}_2\text{SO}_4$ reaction below 240 K, where the formed $\text{HSO}_4 \cdots \text{NH}_3$ complex is thermodynamically favorable. Moreover, it is worth noting that the dominant pathway in the $\text{OH} + \text{H}_2\text{SO}_4 \cdots \text{NH}_3$ reaction is the hydrogen abstraction in H_2SO_4 by OH at low temperatures.

Regarding the $\text{NH}_2 + \text{H}_2\text{SO}_4$ reaction, the calculation results show that the reaction is negligible in the atmosphere. When a single water molecule is introduced to the NH_2 reaction with sulfuric acid, the reaction barrier is reduced to about 10 kcal/mol from 12.33 kcal/mol in the naked reaction of NH_2 with sulfuric acid with respect to the respective pre-reactive complex, which uncovers that a single water molecule assists the $\text{NH}_2 + \text{H}_2\text{SO}_4$ reaction. The calculation results also demonstrate that sulfuric acid containing complexes converted into HSO_4 involving clusters is thermodynamically feasible, which could provide new insights on nucleation processes in the atmosphere.

The rearrangement processes occur in the $\text{OH} + \text{H}_2\text{SO}_4 \cdots \text{NH}_3$, $\text{NH}_2 + \text{H}_2\text{SO}_4$, and $\text{NH}_2 + \text{H}_2\text{SO}_4 \cdots \text{H}_2\text{O}$ reactions. The energy barriers for C1 to M1 A via TS1B, C2B to C2P, CW1B to CW1P, and CW2C to CW2P about are computed to be 9.09 kcal/mol, 4.76 kcal/mol, 8 kcal/mol, 2.37 kcal/mol relative to the respective prereactive complex. The results reflect that these molecular complexes undergo a kinetic bottleneck in their isomerization processes. These results could be of great interest in simulating one to consider nucleation processes from the kinetic point of view, whereas previous investigations on nucleation processes mainly concentrated on the thermodynamic processes and considered the collision rate in the isomerization of molecular clusters.^[79,80] Very recently, experimental and theoretical results have indicated that there is an energy barrier for the addition of ammonia to molecular clusters.^[81–83]

Supporting Information

Supporting information for this article is available on the <http://dx.doi.org/10.1002/slct.201600194>

Acknowledgments

The authors thank the anonymous reviewers for providing valuable comments to improve the article. This research is supported by Science and Technology Foundation of Guizhou Province & Guizhou Minzu University, China ([2014]7380 and [2015]7211), Science and Technology Foundation of Guizhou Provincial Department of Education, China (No. [2015]350).

Keywords: Atmospheric Chemistry · Sulfuric acid · Reaction Mechanisms · Reaction kinetics

- [1] J. G. Calvert, A. Lazrus, G. L. Kok, B. G. Heikes, J. G. Walega, J. Lind, C. A. Cantrell, *Nature*. **1985**, *317*, 27–35.
- [2] M. Sipilä, T. Berndt, T. Petäjä, D. Brus, J. Vanhanen, F. Stratmann, J. Pato-koski, R. L. Mauldin, A.-P. Hyvärinen, H. Lihavainen, M. Kulmala, *Science*. **2010**, *327*, 1243–1246.
- [3] R. J. Weber, G. Chen, D. D. Davis, R. L. Mauldin, D. J. Tanner, F. L. Eisele, A. D. Clarke, D. C. Thornton, A. R. Bandy, *J. Geophys. Res., [Atmos.]*. **2001**, *106*, 24107–24117.
- [4] C. Kuang, P. H. McMurry, A. V. McCormick, F. L. Eisele, *J. Geophys. Res., [Atmos.]*. **2008**, *113*, D10209–.
- [5] R. Zhang, A. Khalizov, L. Wang, M. Hu, W. Xu, *Chem. Rev.* **2012**, *112*, 1957–2011.
- [6] J. Kirkby, J. Curtius, J. Almeida, E. Dunne, J. Duplissy, S. Ehrhart, A. Franchin, S. Gagne, L. Ickes, A. Kurten, A. Kupc, A. Metzger, F. Riccobono, L. Rondo, S. Schobesberger, G. Tsagkogeorgas, D. Wimmer, A. Amorim, F. Bianchi, M. Breitenlechner, A. David, J. Dommen, A. Downard, M. Ehn, R. C. Flagan, S. Haider, A. Hansel, D. Hauser, W. Jud, H. Junninen, F. Kreissl, A. Kvashin, A. Laaksonen, K. Lehtipalo, J. Lima, E. R. Lovejoy, V. Makhmutov, S. Mathot, J. Mikkilä, P. Minginette, S. Mogo, T. Nieminen, A. Onnela, P. Pereira, T. Petaja, R. Schnitzhofer, J. H. Seinfeld, M. Sipilä, Y. Stozhkov, F. Stratmann, A. Tome, J. Vanhanen, Y. Viisanen, A. Vrtala, P. E. Wagner, H. Walther, E. Weingartner, H. Wex, P. M. Winkler, K. S. Carslaw, D. R. Worsnop, U. Baltensperger, M. Kulmala, *Nature*. **2011**, *476*, 429–433.
- [7] I. Riipinen, S. L. Sihto, M. Kulmala, F. Arnold, M. Dal Maso, W. Birmili, K. Saarnio, K. Teinilä, V. M. Kerminen, A. Laaksonen, K. E. J. Lehtinen, *Atmos. Chem. Phys.* **2007**, *7*, 1899–1914.
- [8] S. L. Sihto, M. Kulmala, V. M. Kerminen, M. Dal Maso, T. Petäjä, I. Riipinen, H. Korhonen, F. Arnold, R. Janson, M. Boy, A. Laaksonen, K. E. J. Lehtinen, *Atmos. Chem. Phys.* **2006**, *6*, 4079–4091.
- [9] J. Almeida, S. Schobesberger, A. Kurten, I. K. Ortega, O. Kupiainen-Maatta, A. P. Praplan, A. Adamov, A. Amorim, F. Bianchi, M. Breitenlechner, A. David, J. Dommen, N. M. Donahue, A. Downard, E. Dunne, J. Duplissy, S. Ehrhart, R. C. Flagan, A. Franchin, R. Guida, J. Hakala, A. Hansel, M. Heinritzi, H. Henschel, T. Jokinen, H. Junninen, M. Kajos, J. Kangasluoma, H. Keskinen, A. Kupc, T. Kurten, A. N. Kvashin, A. Laaksonen, K. Lehtipalo, M. Leiminger, J. Leppa, V. Loukonen, V. Makhmutov, S. Mathot, M. J. McGrath, T. Nieminen, T. Olenius, A. Onnela, T. Petaja, F. Riccobono, I. Riipinen, M. Rissanen, L. Rondo, T. Ruuskanen, F. D. Santos, N. Sarnela, S. Schallhart, R. Schnitzhofer, J. H. Seinfeld, M. Simon, M. Sipilä, Y. Stozhkov, F. Stratmann, A. Tome, J. Trostl, G. Tsagkogeorgas, P. Vaattovaara, Y. Viisanen, A. Virtanen, A. Vrtala, P. E. Wagner, E. Weingartner, H. Wex, C. Williamson, D. Wimmer, P. Ye, T. Yli-Juuti, K. S. Carslaw, M. Kulmala, J. Curtius, U. Baltensperger, D. R. Worsnop, H. Vehkamäki, J. Kirkby, *Nature*. **2013**, *502*, 359–363.
- [10] M. Kulmala, T. Petäjä, M. Ehn, J. Thornton, M. Sipilä, D. R. Worsnop, V.-M. Kerminen, *Annu. Rev. Phys. Chem.* **2014**, *65*, 21–37.
- [11] F. Bianchi, A. P. Praplan, N. Sarnela, J. Dommen, A. Kürten, I. K. Ortega, S. Schobesberger, H. Junninen, M. Simon, J. Tröstl, T. Jokinen, M. Sipilä, A. Adamov, A. Amorim, J. Almeida, M. Breitenlechner, J. Duplissy, S. Ehrhart,

- R. C. Flagan, A. Franchin, J. Hakala, A. Hansel, M. Heinritzi, J. Kangasluoma, H. Keskinen, J. Kim, J. Kirkby, A. Laaksonen, M. J. Lawler, K. Lehtipalo, M. Leiminger, V. Makhmutov, S. Mathot, A. Onnela, T. Petäjä, F. Riccobono, M. P. Rissanen, L. Rondo, A. Tomé, A. Virtanen, Y. Viisanen, C. Williamson, D. Wimmer, P. M. Winkler, P. Ye, J. Curtius, M. Kulmala, D. R. Worsnop, N. M. Donahue, U. Baltensperger, *Environ. Sci. Technol.* **2014**, *48*, 13675–13684.
- [12] M. O. Andreae, P. J. Crutzen, *Science*. **1997**, *276*, 1052–1058.
- [13] J. Haywood, O. Boucher, *Rev. Geophys.* **2000**, *38*, 513–543.
- [14] J. T. Kiehl, B. P. Briegleb, *Science*. **1993**, *260*, 311–314.
- [15] Intergovernmental Panel on Climate Change (IPCC): Climate Change 2007: The Physical Science Basis, Cambridge University Press, UK, 2007.
- [16] J. C. Chow, J. G. Watson, J. L. Mauderly, D. L. Costa, R. E. Wyzga, S. Vedal, G. M. Hidy, S. L. Altshuler, D. Marrack, J. M. Heuss, G. T. Wolff, C. Arden Pope III, D. W. Dockery, *J. Air Waste Manage. Assoc.* **2006**, *56*, 1368–1380.
- [17] R. M. Harrison, J. Yin, *Sci. Total Environ.* **2000**, *249*, 85–101.
- [18] A. Valavanidis, K. Fiotakis, T. Vlachogianni, *J. Environ. Sci. Health Part C.* **2008**, *26*, 339–362.
- [19] M. Kulmala, J. Kontkanen, H. Junninen, K. Lehtipalo, H. E. Manninen, T. Nieminen, T. Petäjä, M. Sipilä, S. Schobesberger, P. Rantala, A. Franchin, T. Jokinen, E. Järvinen, M. Äijälä, J. Kangasluoma, J. Hakala, P. P. Aalto, P. Paasonen, J. Mikkilä, J. Vanhanen, J. Aalto, H. Hakola, U. Makkonen, T. Ruuskanen, R. L. Mauldin, J. Duplissy, H. Vehkamäki, J. Bäck, A. Kortelainen, I. Riipinen, T. Kurtén, M. V. Johnston, J. N. Smith, M. Ehn, T. F. Mentel, K. E. J. Lehtinen, A. Laaksonen, V.-M. Kerminen, D. R. Worsnop, *Science*. **2013**, *339*, 943–946.
- [20] J. Elm, M. Fard, M. Bilde, K. V. Mikkelsen, *J. Phys. Chem. A.* **2013**, *117*, 12990–12997.
- [21] J. Zhao, A. Khalizov, R. Zhang, R. McGraw, *J. Phys. Chem. A.* **2009**, *113*, 680–689.
- [22] T. Kurtén, M. R. Sundberg, H. Vehkamäki, M. Noppel, J. Blomqvist, M. Kulmala, *J. Phys. Chem. A.* **2006**, *110*, 7178–7188.
- [23] T. Kurtén, L. Torpo, M. R. Sundberg, V. M. Kerminen, H. Vehkamäki, M. Kulmala, *Atmos. Chem. Phys.* **2007**, *7*, 2765–2773.
- [24] J. Elm, M. Bilde, K. V. Mikkelsen, *J. Chem. Theory Comput.* **2012**, *8*, 2071–2077.
- [25] J. Elm, M. Bilde, K. V. Mikkelsen, *Phys. Chem. Chem. Phys.* **2013**, *15*, 16442–16445.
- [26] L. Torpo, T. Kurtén, H. Vehkamäki, K. Laasonen, M. R. Sundberg, M. Kulmala, *J. Phys. Chem. A.* **2007**, *111*, 10671–10674.
- [27] J. C. Ianni, A. R. Bandy, *J. Phys. Chem. A.* **1999**, *103*, 2801–2811.
- [28] P. Korhonen, M. Kulmala, A. Laaksonen, Y. Viisanen, R. McGraw, J. H. Seinfeld, *J. Geophys. Res., [Atmos.]*. **1999**, *104*, 26349–26353.
- [29] V. Loukonen, T. Kurtén, I. K. Ortega, H. Vehkamäki, A. A. H. Pádua, K. Sellægri, M. Kulmala, *Atmos. Chem. Phys.* **2010**, *10*, 4961–4974.
- [30] T. Kurtén, M. Noppel, H. Vehkamäki, M. Salonen, M. Kulmala, *Boreal Environ. Res.* **2007**, *12*, 431–453.
- [31] W. Zhang, B. Du, Z. Qin, *J. Phys. Chem. A.* **2014**, *118*, 4797–4807.
- [32] J. Elm, M. Bilde, K. V. Mikkelsen, *J. Phys. Chem. A.* **2013**, *117*, 6695–6701.
- [33] F. Stuhl, *J. Chem. Phys.* **1973**, *59*, 635–637.
- [34] M. Monge-Palacios, C. Rangel, J. Espinosa-Garcia, *J. Chem. Phys.* **2013**, *138*, 084305(084301-084314).
- [35] E. W. G. Diau, T. L. Tso, Y. P. Lee, *J. Phys. Chem.* **1990**, *94*, 5261–5265.
- [36] R. Atkinson, D. L. Baulch, R. A. Cox, J. N. Crowley, R. F. Hampson, R. G. Hynes, M. E. Jenkin, M. J. Rossi, J. Troe, *Atmos. Chem. Phys.* **2004**, *4*, 1461–1738.
- [37] J. M. Anglada, S. Olivella, A. Solé, *J. Phys. Chem. A.* **2006**, *110*, 1982–1990.
- [38] J. M. Anglada, S. Olivella, A. Solé, *J. Am. Chem. Soc.* **2014**, *136*, 6834–6837.
- [39] J. M. Anglada, S. Olivella, A. Sole, *Phys. Chem. Chem. Phys.* **2014**, *16*, 19437–19445.
- [40] E. Vöhringer-Martinez, B. Hansmann, H. Hernandez, J. S. Francisco, J. Troe, B. Abel, *Science*. **2007**, *315*, 497–501.
- [41] Z. C. Kramer, K. Takahashi, V. Vaida, R. T. Skodje, *J. Chem. Phys.* **2012**, *136*, 164302–164309.
- [42] V. Vaida, *J. Chem. Phys.* **2011**, *135*, 020901–020908.
- [43] L. Vereecken, J. S. Francisco, *Chem. Soc. Rev.* **2012**, *41*, 6259–6293.
- [44] R. J. Buszek, J. S. Francisco, J. M. Anglada, *Int. Rev. Phys. Chem.* **2011**, *30*, 335–369.
- [45] L. P. Viegas, A. J. C. Varandas, *J. Comput. Chem.* **2014**, *35*, 507–517.
- [46] B. Long, W.-J. Zhang, Z.-W. Long, *Chin. J. Chem. Phys.* **2011**, *24*, 419–424.
- [47] A. J. C. Varandas, *Int. J. Quantum Chem.* **2014**, 1327–1349.
- [48] B. Long, X.-F. Tan, Z.-W. Long, Y.-B. Wang, D.-S. Ren, W.-J. Zhang, *J. Phys. Chem. A.* **2011**, *115*, 6559–6567.
- [49] B. Long, X.-F. Tan, D.-S. Ren, W.-J. Zhang, *J. Mol. Struct.: THEOCHEM.* **2010**, *956*, 44–49.
- [50] M. K. Hazra, J. S. Francisco, A. Sinha, *J. Phys. Chem. A.* **2014**, *118*, 4095–4105.
- [51] C. Iuga, J. Alvarez-Idaboy, A. Vivier-Bunge, *Theor. Chem. Acc.* **2011**, *129*, 209–217.
- [52] C. Iuga, J. R. Alvarez-Idaboy, L. Reyes, A. Vivier-Bunge, *J. Phys. Chem. Lett.* **2010**, *1*, 3112–3115.
- [53] C. Iuga, J. R. Alvarez-Idaboy, A. Vivier-Bunge, *J. Phys. Chem. A.* **2011**, *115*, 5138–5146.
- [54] B. Du, W. Zhang, *J. Phys. Chem. A.* **2013**, *117*, 6883–6892.
- [55] Y. Luo, S. Maeda, K. Ohno, *Chem. Phys. Lett.* **2009**, *469*, 57–61.
- [56] B. Long, Z.-W. Long, Y.-B. Wang, X.-F. Tan, Y.-H. Han, C.-Y. Long, W.-J. Zhang, *ChemPhysChem.* **2012**, *13*, 323–329.
- [57] M. K. Hazra, A. Sinha, *J. Am. Chem. Soc.* **2011**, *133*, 17444–17453.
- [58] M. K. Hazra, J. S. Francisco, A. Sinha, *J. Phys. Chem. A.* **2013**, *117*, 11704–11710.
- [59] A. Kürten, S. Münch, L. Rondo, F. Bianchi, J. Duplissy, T. Jokinen, H. Junninen, N. Sarnela, S. Schobesberger, M. Simon, M. Sipilä, J. Almeida, A. Amorim, J. Dommen, N. M. Donahue, E. M. Dunne, R. C. Flagan, A. Franchin, J. Kirkby, A. Kupc, V. Makhmutov, T. Petäjä, A. P. Praplan, F. Riccobono, G. Steiner, A. Tomé, G. Tsagkogeorgas, P. E. Wagner, D. Wimmer, U. Baltensperger, M. Kulmala, D. R. Worsnop, J. Curtius, *Atmos. Chem. Phys.* **2015**, *15*, 10701–10721.
- [60] D. R. Hanson, F. Eisele, *J. Phys. Chem. A.* **2000**, *104*, 1715–1719.
- [61] E. C. Tuazon, A. M. Winer, J. N. Pitts, *Environ. Sci. Technol.* **1981**, *15*, 1232–1237.
- [62] W. P. Robarge, J. T. Walker, R. B. McCulloch, G. Murray, *Atmos. Environ.* **2002**, *36*, 1661–1674.
- [63] M. Monge-Palacios, J. C. Corchado, J. Espinosa-Garcia, *J. Chem. Phys.* **2013**, *138*, 214306(214301-214311).
- [64] B. Long, W.-J. Zhang, X.-F. Tan, Z.-W. Long, Y.-B. Wang, D.-S. Ren, *J. Phys. Chem. A.* **2011**, *115*, 1350–1357.
- [65] D. L. Fiacco, S. W. Hunt, K. R. Leopold, *J. Am. Chem. Soc.* **2002**, *124*, 4504–4511.
- [66] M. Torrent-Sucarrat, J. S. Francisco, J. M. Anglada, *J. Am. Chem. Soc.* **2012**, *134*, 20632–20644.
- [67] B. Long, X.-F. Tan, C.-R. Chang, W.-X. Zhao, Z.-W. Long, D.-S. Ren, W.-J. Zhang, *J. Phys. Chem. A.* **2013**, *117*, 5106–5116.
- [68] L. Partanen, V. Hänninen, L. Halonen, *J. Phys. Chem. A.* **2012**, *116*, 2867–2879.
- [69] J. Clark, S. Kumbhani, J. C. Hansen, J. S. Francisco, *J. Chem. Phys.* **2011**, *135*, 244305(1-11).
- [70] J. M. Anglada, *J. Am. Chem. Soc.* **2004**, *126*, 9809–9820.
- [71] J. M. Anglada, J. Gonzalez, *ChemPhysChem.* **2009**, *10*, 3034–3045.
- [72] S. Olivella, J. M. Anglada, A. Solé, J. M. Bofill, *Chem.—Eur. J.* **2004**, *10*, 3404–3410.
- [73] J. Gonzalez, J. M. Anglada, *J. Phys. Chem. A.* **2010**, *114*, 9151–9162.
- [74] B. Wang, Z. Cao, *Angew. Chem. Int. Ed.* **2011**, *50*, 3266–3270.
- [75] M. Torrent-Sucarrat, M. F. Ruiz-Lopez, M. Martins-Costa, J. S. Francisco, J. M. Anglada, *Chem.—Eur. J.* **2011**, *17*, 5076–5085.
- [76] R. J. Shannon, M. A. Blitz, A. Goddard, D. E. Heard, *Nat Chem.* **2013**, *5*, 745–749.
- [77] G.-L. Hou, W. Lin, S. H. M. Deng, J. Zhang, W.-J. Zheng, F. Paesani, X.-B. Wang, *J. Phys. Chem. Lett.* **2013**, *4*, 779–785.
- [78] J. Herb, Y. Xu, F. Yu, A. B. Nadykto, *J. Phys. Chem. A.* **2012**, *117*, 133–152.
- [79] H. Vehkamäki, I. Riipinen, *Chem. Soc. Rev.* **2012**, *41*, 5160–5173.
- [80] P. Paasonen, T. Olenius, O. Kupiainen, T. Kurtén, T. Petäjä, W. Birmili, A. Hamed, M. Hu, L. G. Huey, C. Plass-Dueller, J. N. Smith, A. Wiedensohler, V. Loukonen, M. J. McGrath, I. K. Ortega, A. Laaksonen, H. Vehkamäki, V. M. Kerminen, M. Kulmala, *Atmos. Chem. Phys.* **2012**, *12*, 9113–9133.
- [81] J. W. DePalma, B. R. Bzdek, D. P. Ridge, M. V. Johnston, *J. Phys. Chem. A.* **2014**, *118*, 11547–11554.
- [82] B. R. Bzdek, J. W. DePalma, D. P. Ridge, J. Laskin, M. V. Johnston, *J. Am. Chem. Soc.* **2013**, *135*, 3276–3285.
- [83] T. Olenius, O. Kupiainen-Määttä, I. K. Ortega, T. Kurtén, H. Vehkamäki, *J. Chem. Phys.* **2013**, *139*, 084312(1-12).

Submitted: March 11, 2016

Accepted: April 29, 2016
